# Supporting Information

# Robust N-doped Carbon Aerogels Strongly Coupled with Iron-Cobalt Particles as Efficient Bifunctional Catalysts for Rechargeable Zn–Air Batteries

Gengtao Fu,[a] Yu Liu,[a] Yifan Chen,[c] Yawen Tang,[c] John B. Goodenough[b,*], Jong-Min Lee[a,*]

[a] School of Chemical and Biomedical Engineering, Nanyang Technological University, Singapore 637459, Singapore. E-mail: jmlee@ntu.edu.sg

[b] Materials Science and Engineering Program & Texas Materials Institute, The University of Texas at Austin, Austin, Texas 78712, United States. E-mail: jgoodenough@mail.utexas.edu

[c] Jiangsu Key Laboratory of New Power Batteries, Jiangsu Collaborative Innovation Center of Biomedical Functional Materials, School of Chemistry and Materials Science, Nanjing Normal University, Nanjing 210023, China.

## Part I: Experimental

### Materials and reagents

Potassium hexacyanoferrate(II) ($K_4Fe(CN)_6$), potassium hexacyanocobaltate (III) ($K_3Co(CN)_6$), chitosan (CS, 85% deacetylate) were purchased from Alfa Aesar. Graphene oxided was purchased from Nanjing XFNANO Materials Tech Co., Ltd. Commercial 20% Pt/C and $RuO_2$ were purchased from Johnson Matthey Chemicals Ltd. All reagents and chemicals were used without further purification.

### Synthesis of 3D Porous FeCo/N-DNC Aerogels

Typically, 1 ml $K_4Fe(CN)_6$ (0.50 M) and 1 ml $K_3Co(CN)_6$ (0.50 M) aqueous solutions were mixed at room temperature. It was then mixed with a 20 mL aqueous solution containing chitosan (10 mg ml$^{-1}$) and 20 mg GO. After continuous ultrasonic for 5 min, the homogeneous $K_4Fe(CN)_6$/$K_3Co(CN)_6$-CS-GO hydrogel was formed. Subsequently, the $K_4Fe(CN)_6$/$K_3Co(CN)_6$-CS-GO aerogel was obtained through a freeze-drying process (20 h) by using the $K_4Fe(CN)_6$/$K_3Co(CN)_6$-CS-GO hydrogel as a precursor that was annealed at 600 °C for 3 h in $H_2$ at a heating rate of 5 °C min$^{-1}$. Once cooled down to room temperature, the obtained loose product was washed with distilled water and absolute alcohol several times and subsequently dried at 60 °C to yield the FeCo/N-DNC aerogels.

### Physicochemical characterization

The phase purity and crystallinity of the products were identified by X-ray powder diffraction (XRD) on a Rigaku MiniFlex 600 I diffractometer with Cu Kα radiation (λ = 0.15406 nm). Thermogravimetric analysis (TGA) of the samples was carried out with a Perkin-Elmer thermal analysis system. Measurements were made by heating from 40 to 800 $^{o}C$ at a heating rate of 10 $^{o}C$ $min^{-1}$ under air atmosphere. X-ray photoelectron spectroscopy (XPS) was carried out on a Thermo VG Scientific ESCALAB 250 spectrometer with an Al Kα radiator. The binding energy was calibrated by means of the C 1s peak energy of 284.6 eV. Raman spectra were recorded on a Raman spectrometer (LabRAM HR800, λ=514 nm). Scanning electron microscopy (SEM) and energy dispersive X-ray analysis (EDX) were performed with a Hitachi S5500 SEM/STEM. Transmission electron microscopy (TEM) and scanning transmission electron microscopy (STEM) were performed with a JEOL 2010F TEM/STEM operated at 200 kV. The $N_2$ adsorption-desorption experiment was operated at 77 K on a Micromeritics ASAP 2050 system. The pore size distributions were measured with a Barret-Joyner-Halenda (BJH) model. The electrical conductivity was measured with 4-probe conductivity measurements on ST-2722 semiconductor resistivity of the powder tester (Suzhou Jingge Electronic Co., Ltd., PR China) under a pressure of 10 MPa.

**Electrochemical Measurements**

Electrochemical measurements were carried out with a CHI 760E electrochemical analyzer (Shanghai, Chenghua Co.). A standard three-electrode system was used, including a rotating disk electrode (RDE) as the working electrode (0.196 $cm^2$), a platinum wire as the auxiliary electrode, and a Ag/AgCl (1 M NaCl) electrode as the reference electrode. All potentials are reported versus the reversible hydrogen electrode (RHE), and for conversion of the obtained potential (vs. Ag/AgCl) to RHE; the following equation was used: $E_{RHE} = E_{Ag/AgCl} + 0.0592\ pH + E_{Ag/AgCl}^{0}$; {$E_{Ag/AgCl}^{0}$ (in 1 M KCl) = +0.235 V; pH = 12.9 for 0.1 M KOH}.

The catalyst ink was prepared by ultrasonically dispersing a mixture of 5 mg of catalyst, 1 mL ethanol, and 20 μL of 5 wt.% Nafion solution. 10 μL of the catalyst ink was pipetted and spread onto the electrode. The loading of the studied catalysts was 250 μg $cm^{-2}$. For the ORR test, the background current was measured under $N_2$ atmosphere at the identical rotation speed and scan rate as conducted under $O_2$. The ORR activities of the catalysts were measured via the RDE voltammograms in a 0.1 M KOH electrolyte at predefined rotation rates and a scan rate of 5 mV $s^{-1}$. Before testing, $O_2$ was passed through the electrolyte for at least 20 min to saturate the electrolyte with $O_2$. To remove the capacitive current of the working electrode, the background current was measured by running the above electrodes in $N_2$-saturated 0.1 M KOH and then subtracted from the ORR polarization curve. For the OER, the polarization curves were recorded from 1.1 to 2.0 V at a scan rate of 5 mV $s^{-1}$ with a rotation speed of 1600 rpm to spin off the oxygen evolved during the testing.

**Zn-air Battery Measurements**

The Zn–air battery tests were performed with a homemade Zn-air cell. The air cathode consisted of the hydroholic carbon paper with a gas diffusion layer on the air-facing side and a catalyst layer on the water-facing side. The catalyst layer was made by loading the catalyst ink onto the carbon paper by drop-casting, with a loading of 10 mg $cm^{-2}$ for all the catalysts. A polished Zn plate with a thickess of 0.3 mm was used as the anode. A 0.2 M $ZnCl_2$ + 6 M KOH mixed solution was used as the electrolyte.

The gas diffusion layer has an effective area of 0.5 $cm^2$ and allows $O_2$ from ambient air to reach the catalyst sites. A Land CT2001A system was used to carry out the cycling test with a five-minute rest time between each discharge and charge at a current density of 10 mA $cm^{-2}$. Each discharge and charge period were set to be 10 min. Based on the discharge curves at a constant current density of 5 mA $cm^{-2}$, we can calculate the corresponding specific capacity (mAh $g_{Zn}^{-1}$) and energy density (Wh $kg_{Zn}^{-1}$) by the following equations, respectively.

$$Specific\ capacity\ = \frac{current\ \times service\ hours}{weight\ of\ consumed\ Zn}$$

$$Energy\ density\ = \frac{current\ \times service\ hours\ \times average\ discharge\ voltage}{weight\ of\ consumed\ Zn}$$

## Part I: Figures and Tables

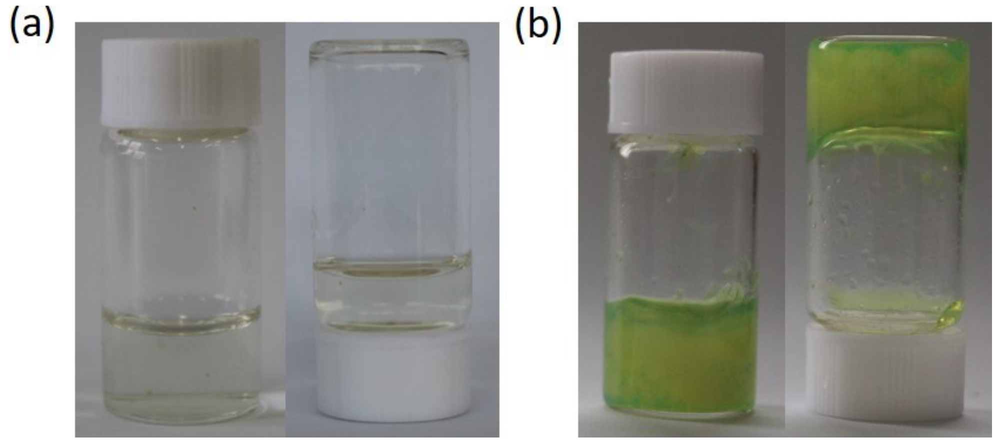


**Fig. S1** The photographs of (a) CS solution and (b) $K_4Fe(CN)_6$/$K_3Co(CN)_6$-CS hydrogel.

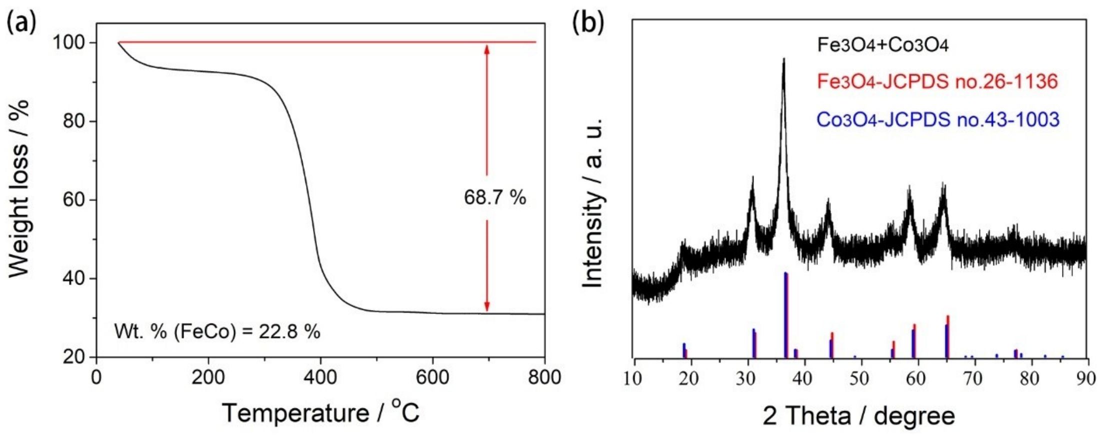


**Fig. S2** (a) TGA curve of FeCo/N-DNC aerogels; (b) XRD pattern of FeCo/N-DNC aerogels after TGA measurement.

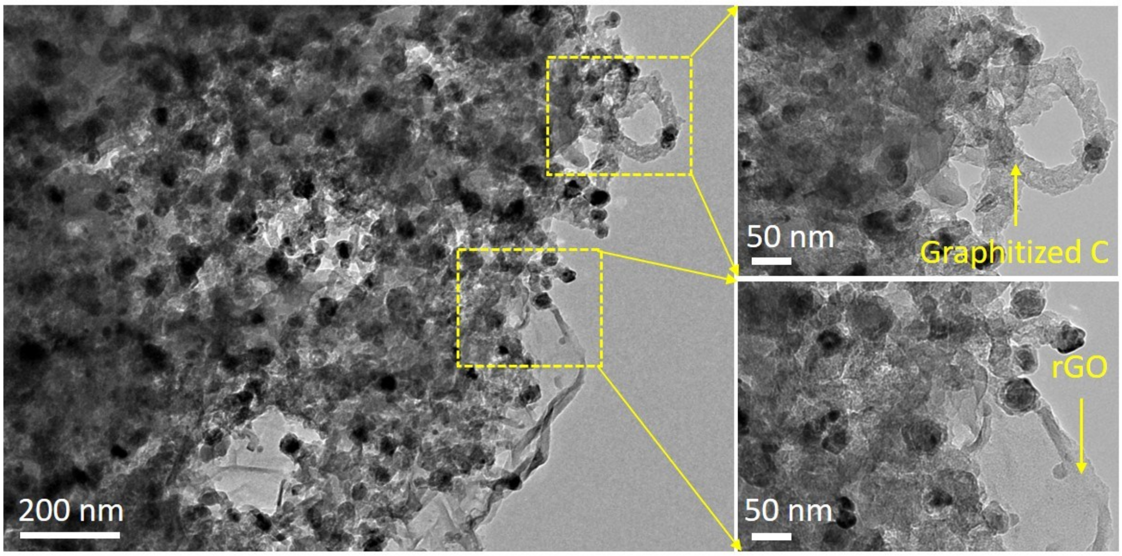


**Fig. S3** TEM images of FeCo/N-DNC aerogels at different magnifications.

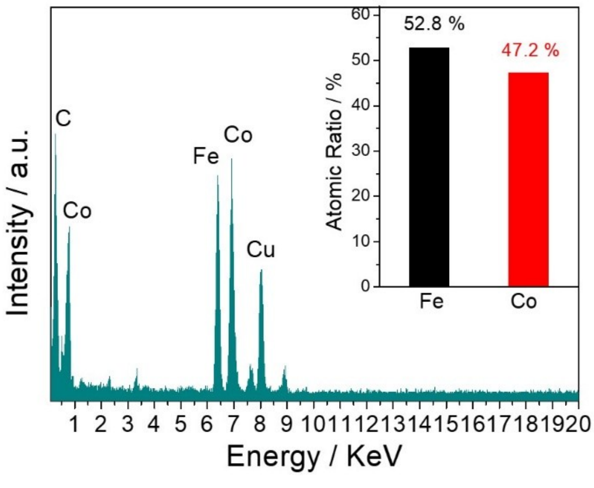


**Fig. S4** EDX spectrum of FeCo/N-DNC aerogels and corresponding atom contents.

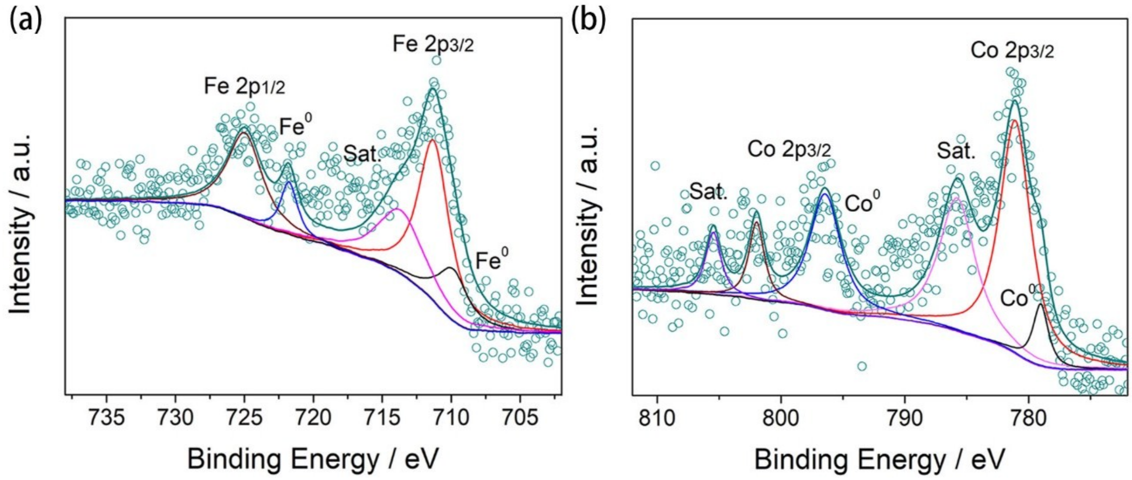


**Fig. S5** High-resolution XPS spectra of (a) Fe 2p and (b) Co 2p core levels in FeCo/N-DNC aerogels.

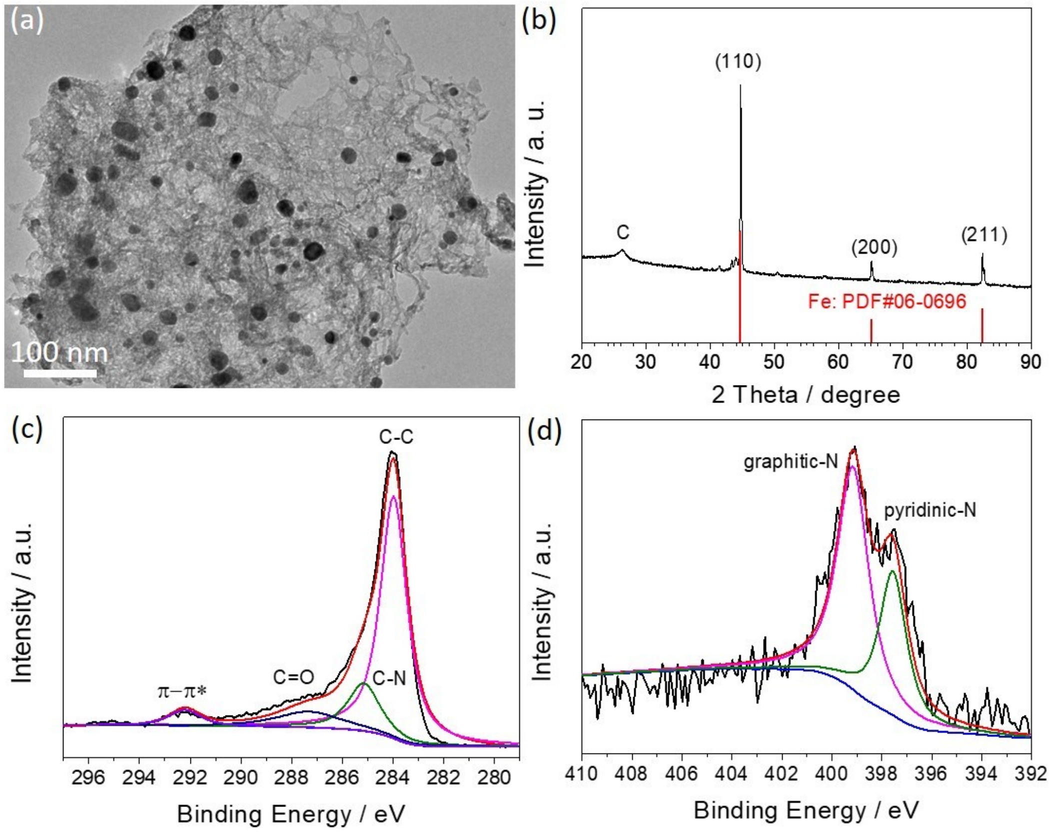


**Fig. S6** (a) TEM image and (b) XRD pattern of Fe/N-DNC aerogels; (c) High-resolution XPS spectra of (c) C 1s and (d) N 1s core levels.

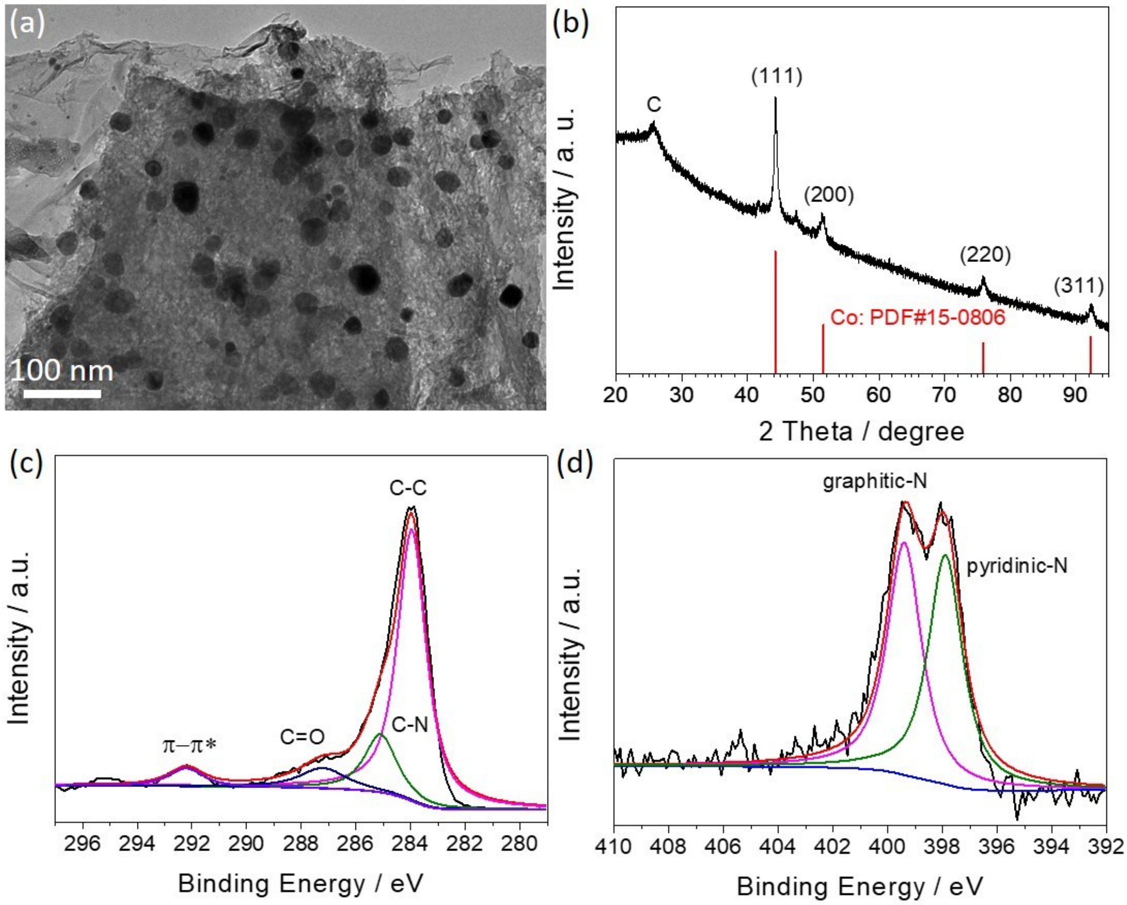


**Fig. S7** (a) TEM image and (b) XRD pattern of Co/N-DNC aerogels; (c) High-resolution XPS spectra of (c) C 1s and (d) N 1s core levels.

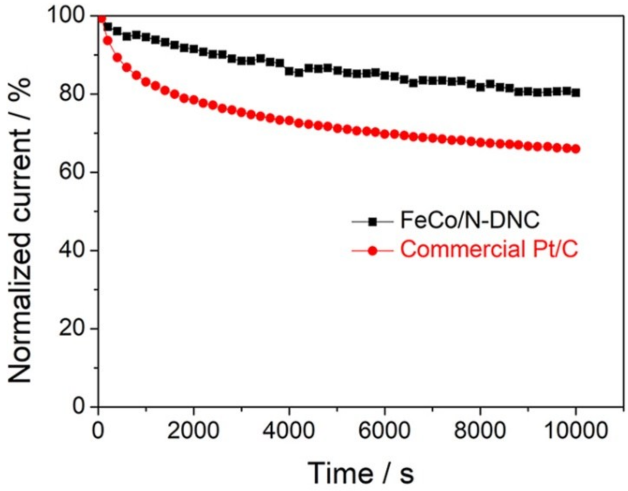


**Fig. S8** Chronoamperometric responses of catalysts at 0.7 V in $O_2$-saturated 0.1 M KOH (percentage of current retained versus operation time).

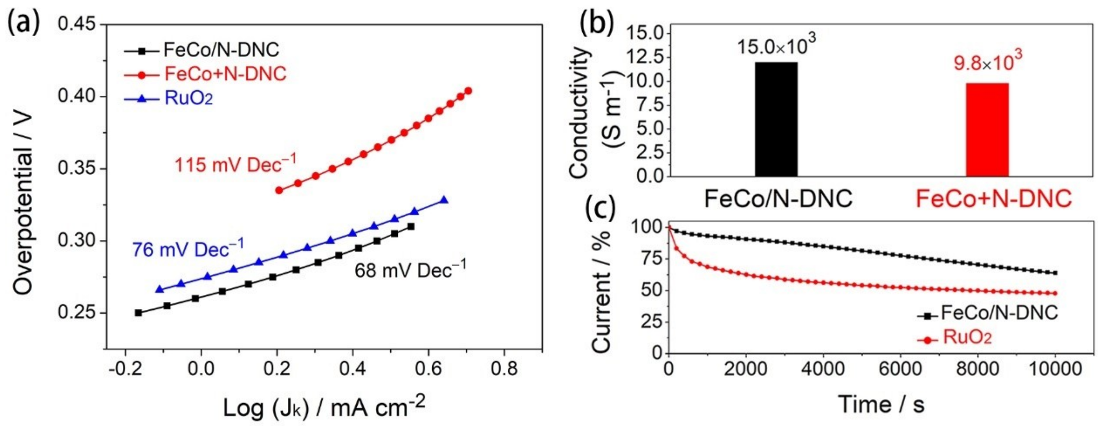


**Fig. S9** (a) Tafel plots derived from Figure 6a; (b) Electrical conductivity of FeCo/N-DNC aerogels and mixed FeCo+N-DNC aerogels; (c) Chronoamperometric responses of FeCo/N-DNC aerogels and $RuO_2$ catalysts at 1.65 V in $O_2$-saturated 0.1 M KOH;

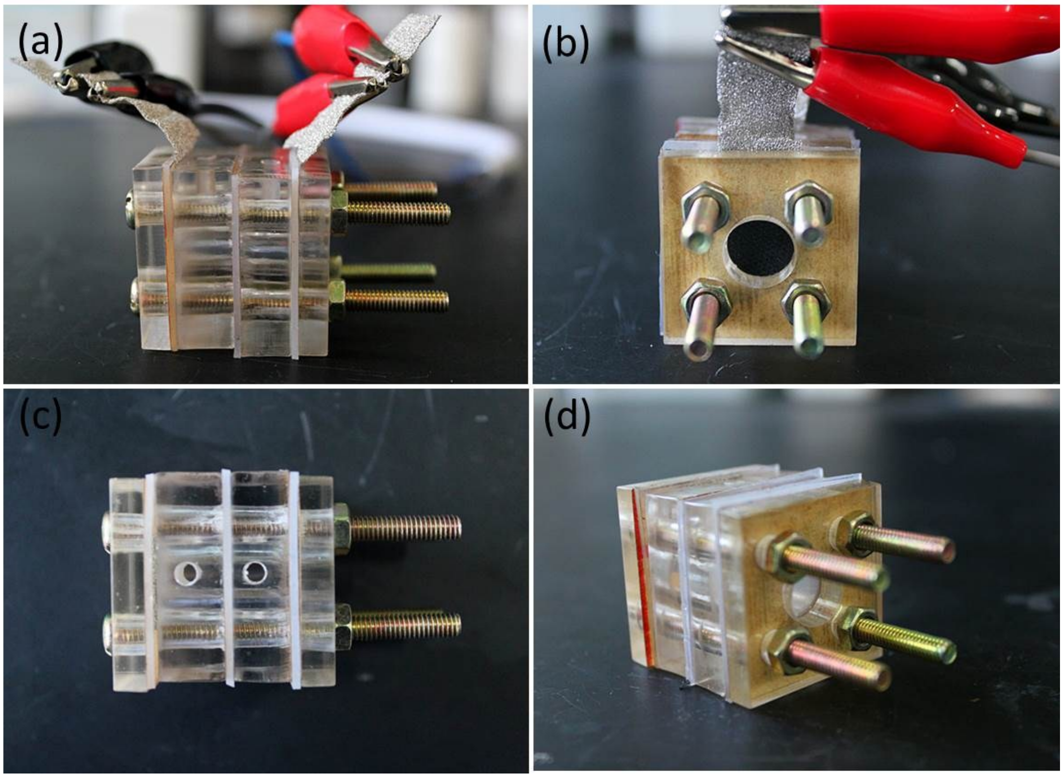


**Fig. S10** Digital images of the rechargeable Zn-air battery recorded from the different directions.

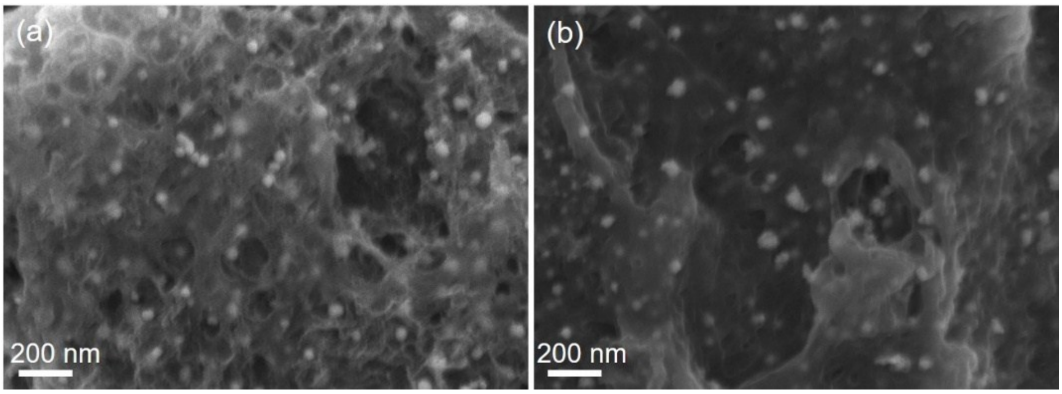


**Fig. S11** SEM images of FeCo/N-DNC aerogels (a) before and (b) after the charge/discharge cycles.

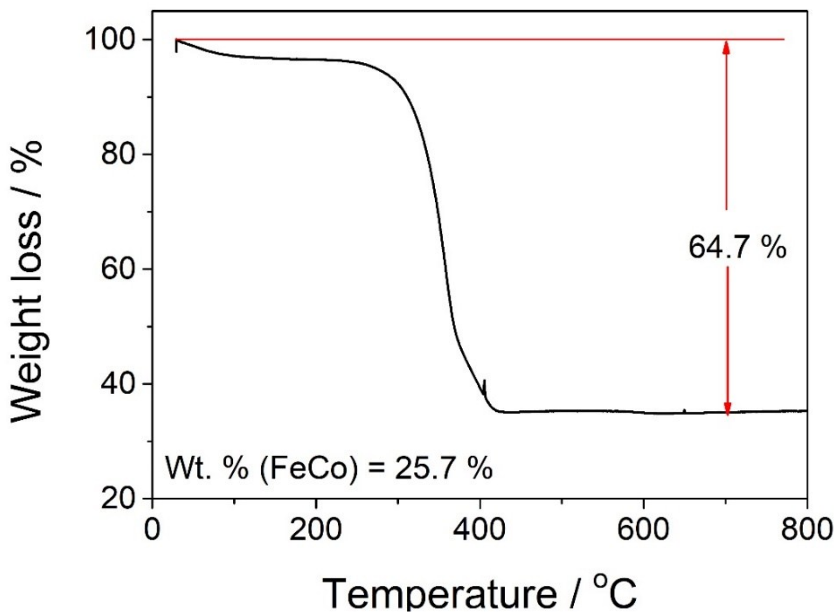

**Fig. S12** TGA curve of FeCo/N-DNC aerogels after the charge/discharge cycles.

**Table S1**. Comparison of the ORR activity of FeCo/N-DNC aerogels with other ORR catalysts previously reported.

| Number | Catalyst | $E_{1/2}$ / V | Electrolyte | Loadings (mg $cm^{-2}$) | Ref |
|---|---|---|---|---|---|
| 1 | FeCo/N-DNC | 0.81 | 0.1 M KOH | 0.25 | this work |
| 2 | Mo–N/C@$MoS_2$ | 0.81 | 0.1 M KOH | ~ | [1] |
| 3 | BFNCNTs | 0.81 | 0.1 M KOH | 0.75 | [2] |
| 4 | FeCo@NC-750 | 0.80 | 0.1 M KOH | 0.80 | [3] |
| 5 | $Co_3O_4$/N-rGO | 0.79 | 0.1 M KOH | 0.128 | [4] |
| 6 | N, S-CN | 0.77 | 0.1 M KOH | 0.20 | [5] |
| 7 | Co/CoOx | 0.76 | 0.1 M KOH | 0.51 | [6] |
| 8 | NiCo@N-C-3 | 0.76 | 0.1 M KOH | 0.4 | [7] |
| 9 | Co/N-C-800 | 0.74 | 0.1 M KOH | 0.25 | [8] |
| 10 | Mn oxide | 0.73 | 0.1 M KOH | ~ | [9] |
| 11 | $NiCo_2S_4$@N/S-rGO | 0.72 | 0.1 M KOH | 0.283 | [10] |
| 12 | NGSH | 0.70 | 0.1 M KOH | 0.26 | [11] |
| 13 | N-graphene/CNT | 0.69 | 0.1 M KOH | 0.20 | [12] |
| 14 | $NiCo_2S_4$/CNT | 0.69 | 1.0 M KOH | 0.248 | [13] |
| 15 | NiO/CoN | 0.68 | 0.1 M KOH | 0.20 | [14] |
| 16 | $Co_3O_4$/2.7$Co_2MnO_4$ | 0.68 | 0.1 M KOH | 0.09 | [15] |
| 17 | PCN–CFP | 0.67 | 0.1 M KOH | 0.20 | [16] |
| 18 | $NiCo_2O_4$/G | 0.56 | 0.1 M KOH | 0.41 | [17] |

**Table S2**. Comparison of the OER activity of FeCo/N-DNC aerogels with other OER catalysts previously reported.

| Number | Catalyst | Overpotential / V (10 mA cm$^{-2}$) | Electrolyte | Catalyst loadings (mg cm$^{-2}$) | Ref |
|---|---|---|---|---|---|
| 1 | FeCo/N-DNC | 0.39 | 0.1 M KOH | 0.25 | this work |
| 2 | Fe-$N_4$ SAs/NPC | 0.202 | 0.1 M KOH | ~ | [18] |
| 3 | 5.0%Ce-NiFe-LDH/CNT | 0.227 | 1 M KOH | 0.2 | [19] |
| 4 | RuP/NPC | 0.31 | 1 M KOH | 0.21 | [20] |
| 5 | CoNi@NCNT/NF | 0.31 | 0.1 M KOH | 0.408 | [21] |
| 6 | CoNi-NS/rGO | 0.33 | 1 M KOH | 1.0 | [22] |
| 7 | CoSx@PCN/rGO | 0.34 | 0.1 M KOH | 0.408 | [23] |
| 8 | C-MOF-C2-900 | 0.35 | 0.1 M KOH | 0.2 | [24] |
| 9 | NNU-23 | 0.365 | 0.1 M KOH | 1.0 | [25] |
| 10 | Co@$Co_3O_4$@NC-900 | 0.37 | 0.1 M KOH | ~ | [26] |
| 11 | FeCo-Nx-CN-30 | 0.37 | 0.1 M KOH | 0.1 | [27] |
| 12 | 20% Ir/C | 0.38 | 0.1 M KOH | 0.14 | [9] |
| 13 | $CoS_2$(400)/N, S-GO | 0.38 | 0.1 M KOH | 0.53 | [28] |
| 14 | NCNT/CoO-Co | 0.38 | 1.0 M KOH | 0.21 | [29] |
| 15 | Co/N-CNT | 0.39 | 0.1 M KOH | 0.20 | [30] |
| 16 | CoZn-NC-700 | 0.39 | 0.1 M KOH | 0.24 | [31] |
| 17 | 20% Ru/C | 0.39 | 0.1 M KOH | 0.14 | [9] |
| 18 | FeNx-embedded PNC | 0.395 | 0.1 M KOH | 0.14 | [32] |
| 19 | NiCo/NLG-270 | 0.4 | 1.0 M KOH | 0.4 | [33] |
| 20 | NiCo/PFC aerogels | 0.40 | 0.1 M KOH | 0.13 | [34] |
| 21 | NGSH | 0.40 | 0.1 M KOH | 0.26 | [11] |
| 22 | PCN–CFP | 0.4 | 0.1 M KOH | 0.20 | [16] |
| 23 | NC@Co-NGC DSNC | 0.41 | 0.1 M KOH | 0.40 | [35] |
| 24 | N-graphene/CNT | 0.42 | 0.1 M KOH | 0.20 | [12] |
| 25 | TiC-carbon nitride | 0.42 | 0.1 M KOH | 1.40 | [36] |
| 26 | Co@$Co_3O_4$/NC-1 | 0.42 | 0.1 M KOH | 0.21 | [37] |
| 27 | N, S-CN | 0.45 | 0.1 M KOH | 0.20 | [5] |
| 28 | $NiCo_2O_4$-graphene | 0.46 | 0.1 M KOH | 2.00 | [38] |
| 29 | CCH-2/C | 0.51 | 0.1 M KOH | 0.18 | [39] |
| 30 | NiCo@N-C | 0.53 | 0.1 M KOH | 0.4 | [7] |
| 31 | Mn oxide | 0.54 | 0.1 M KOH | ~ | [9] |
| 32 | $Co_3O_4$/2.7$Co_2MnO_4$ | 0.54 | 0.1 M KOH | 0.09 | [15] |

**Table S3**. Comparison of the performances of Zn-air batteries with various bifunctional electrocatalysts.

| **Catalyst** | **Electrolyte** | **Specific capacity ($mAh\ g_{Zn}^{-1}$)** | **Energy density ($Wh\ kg_{Zn}^{-1}$)** | **Cycle Condition ($mA\ cm^{-2}$)** | **Ref** |
|---|---|---|---|---|---|
| FeCo/N-DNC | 6.0 M KOH + 0.20 M $ZnCl_2$ | 804 | 988 | 5 | This work |
| Pt/C + $RuO_2$ | 6.0 M KOH + 0.20 M $ZnCl_2$ | 699 | 870 | 5 | This work |
| BHPC-950 | 6.0 M KOH | 797 | 963 | 20 | 40 |
| Mo–N/C@$MoS_2$ | 6.0 M KOH + 0.20 M $Zn(Ac)_2$ | ~ | 846.07 | 5 | 1 |
| NGM-Co | 6.0 M KOH + 0.20 M $ZnCl_2$ | 750 | 840 | 2 | 41 |
| NPMC-1000 | 6.0 M KOH | 735 | 835 | 2 | 42 |
| CNT/graphene | 6.0 M KOH | 712 | 872 | 5 | 43 |
| Porous C fiber film | 6.0 M KOH + 0.20 M $Zn(Ac)_2$ | 660 | 838 | 5 | 44 |
| NCNF | 6.0 M KOH + 0.20 M $ZnCl_2$ | 626 | 776 | 10 | 45 |
| Porous C fiber film | 6.0 M KOH + 0.20 M $Zn(Ac)_2$ | 626 | 776 | 10 | 44 |
| NCNT/CoO-NiONiCo | 6.0 M KOH + 0.20 M $ZnCl_2$ | 594 | 713 | 7 | 29 |
| NCO-$A_1$ | 6.0 M KOH | 580 | ~ | 20 | 46 |
| NCNF/$Co_xMn_{1-x}O$ | 6.0 M KOH + 0.20 M $ZnCl_2$ | 581 | 695 | 7 | 47 |
| Ag-Cu on Ni foam | 6.0 M KOH + 0.20 M $ZnCl_2$ | 572 | 641 | 20 | 48 |
| CoO/N-CNT+NiFe LDH | 6.0 M KOH + 0.20 M $ZnCl_2$ | 570 | 700 | 20 | 49 |
| CoZn-NC-700 | 6.0 M KOH + 0.10 M $ZnCl_2$ | 578 | 694 | 10 | 31 |
| $Ni_3Fe$/N-C | 6.0 M KOH + 0.20 M $ZnCl_2$ | 528 | 634 | 10 | 50 |
| $Co_3O4$/N-rGO | 6.0 M KOH + 0.20 M $ZnCl_2$ | 550 | 649 | 6 | 4 |
| NCNT/CoO-NiONiCo | 6.0 M KOH + 0.20 M $ZnCl_2$ | 545 | 615 | 20 | 29 |
| $NiCo_2S_4$/N-CNT | 6.0 M KOH + 0.20 M $ZnCl_2$ | 431.1 | 554.6 | 10 | 13 |

## Part II: References


1. I. S. Amiinu, Z. Pu, X. Liu, K. A. Owusu, H. G. R. Monestel, F. O. Boakye, H. Zhang and S. Mu, *Adv. Funct. Mater.*, 2017, **27**, 1702300.

2. R. Nandan and K. K. Nanda, *J. Mater. Chem. A*, 2017, **5**, 16843-16853.

3. P. Cai, S. Ci, E. Zhang, P. Shao, C. Cao and Z. Wen, *Electrochim. Acta*, 2016, **220**, 354-362.

4. Y. Li, C. Zhong, J. Liu, X. Zeng, S. Qu, X. Han, Y. Deng, W. Hu and J. Lu, *Adv. Mater.*, 2017, **30**, 1703657.

5. K. Qu, Y. Zheng, S. Dai and S. Z. Qiao, *Nano Energy*, 2016, **19**, 373-381.

6. B. Hua, M. Li, Y.-F. Sun, Y.-Q. Zhang, N. Yan, J. Chen, T. Thundat, J. Li and J.-L. Luo, *Nano Energy*, 2017, **32**, 247-254.

7. Y. Fu, H.-Y. Yu, C. Jiang, T.-H. Zhang, R. Zhan, X. Li, J.-F. Li, J.-H. Tian and R. Yang, *Adv. Funct. Mater.*, 2018, **28**, 1705094.

8. Y. Su, Y. Zhu, H. Jiang, J. Shen, X. Yang, W. Zou, J. Chen and C. Li, *Nanoscale*, 2014, **6**, 15080-15089.

9. Y. Gorlin and T. F. Jaramillo, *J. Am. Chem. Soc.*, 2010, **132**, 13612-13614.

10. Q. Liu, J. Jin and J. Zhang, *ACS Appl. Mater. interfaces*, 2013, **5**, 5002-5008.

11. G. L. Tian, M. Q. Zhao, D. Yu, X. Y. Kong, J. Q. Huang, Q. Zhang and F. Wei, *Small*, 2014, **10**, 2251-2259.

12. Z. Wen, S. Ci, Y. Hou and J. Chen, *Angew. Chem. Int. Ed.*, 2014, **53**, 6496-6500.

13. X. Han, X. Wu, C. Zhong, Y. Deng, N. Zhao and W. Hu, *Nano Energy*, 2017, **31**, 541-550.

14. J. Yin, Y. Li, F. Lv, Q. Fan, Y.-Q. Zhao, Q. Zhang, W. Wang, F. Cheng, P. Xi and S. Guo, *ACS Nano*, 2017, **11**, 2275-2283.

15. D. Wang, X. Chen, D. G. Evans and W. Yang, *Nanoscale*, 2013, **5**, 5312-5315.

16. T. Y. Ma, J. Ran, S. Dai, M. Jaroniec and S. Z. Qiao, *Angew. Chem. Int. Ed.*, 2015, **54**, 4646-4650.

17. D. U. Lee, B. J. Kim and Z. Chen, *J. Mater. Chem. A*, 2013, **1**, 4754-4762.

18. Y. Pan, S. Liu, K. Sun, X. Chen, B. Wang, K. Wu, X. Cao, W.-C. Cheong, R. Shen

and A. Han, *Angew. Chem. Int. Ed.*, 2018, **130**, 8750-8754.
19. H. Xu, B. Wang, C. Shan, P. Xi, W. Liu and Y. Tang, *ACS Appl. Mater. interfaces*, 2018, **10**, 6336-6345.
20. Q. Qin, H. Jang, L. Chen, G. Nam, X. Liu and J. Cho, *Adv. Energy Mater.*, 2018, **0**, 1801478.
21. W. Niu, S. Pakhira, K. Marcus, Z. Li, J. L. Mendoza-Cortes and Y. Yang, *Adv. Energy Mater.*, 2018, **8**, 1800480.
22. T. Wang, J. Wu, Y. Liu, X. Cui, P. Ding, J. Deng, C. Zha, E. Coy and Y. Li, *Energy Stor. Mater.*, 2018, **16**, 24-30.
23. W. Niu, Z. Li, K. Marcus, L. Zhou, Y. Li, R. Ye, K. Liang and Y. Yang, *Adv. Energy Mater.*, 2018, **8**, 1701642.
24. M. Zhang, Q. Dai, H. Zheng, M. Chen and L. Dai, *Adv. Mater.*, 2018, **30**, 1705431.
25. W. Xiao-Li, D. Long-Zhang, Q. Man, T. Yu-Jia, L. Jiang, L. Yafei, L. Shun-Li, S. Jia-Xin and L. Ya-Qian, *Angew. Chem. Int. Ed.*, 2018, **57**, 9660-9664.
26. Z. Guo, F. Wang, Y. Xia, J. Li, A. G. Tamirat, Y. Liu, L. Wang, Y. Wang and Y. Xia, *J. Mater. Chem. A*, 2018, 6, 1443-1453.
27. S. Li, C. Cheng, X. Zhao, J. Schmidt and A. Thomas, *Angew. Chem. Int. Ed.*, 2018, **130**, 1874-1880.
28. P. Ganesan, M. Prabu, J. Sanetuntikul and S. Shanmugam, *ACS Catal.*, 2015, **5**, 3625-3637.
29. X. Liu, M. Park, M. G. Kim, S. Gupta, G. Wu and J. Cho, *Angew. Chem. Int. Ed.*, 2015, **54**, 9654-9658.
30. Y. Liu, H. Jiang, Y. Zhu, X. Yang and C. Li, *J. Mater. Chem. A*, 2016, **4**, 1694-1701.
31. B. Chen, X. He, F. Yin, H. Wang, D. J. Liu, R. Shi, J. Chen and H. Yin, *Adv. Funct. Mater.*, 2017, **27**, 1700795.
32. L. Ma, S. Chen, Z. Pei, Y. Huang, G. Liang, F. Mo, Q. Yang, J. Su, Y. Gao and J. Zapien, *ACS nano*, 2018, **12**, 1949–1958.
33. X. R. Wang, J. Y. Liu, Z. W. Liu, W. C. Wang, J. Luo, X. P. Han, X. W. Du, S. Z. Qiao and J. Yang, *Adv. Mater.*, 2018, **30**, 1800005.

34. G. Fu, Y. Chen, Z. Cui, Y. Li, W. Zhou, S. Xin, Y.-w. Tang and J. B. Goodenough, *Nano Lett.*, 2016, **16**, 6516–6522.

35. S. Liu, Z. Wang, S. Zhou, F. Yu, M. Yu, C.-Y. Chiang, W. Zhou, J. Zhao and J. Qiu, *Adv. Mater.*, 2017, **29**, 1700874.

36. T. Y. Ma, J. L. Cao, M. Jaroniec and S. Z. Qiao, *Angew. Chem. Int. Ed.*, 2016, **55**, 1138-1142.

37. A. Aijaz, J. Masa, C. Rösler, W. Xia, P. Weide, A. J. Botz, R. A. Fischer, W. Schuhmann and M. Muhler, *Angew. Chem. Int. Ed.*, 2016, **55**, 4087 –4091.

38. S. Chen and S.-Z. Qiao, *ACS Nano*, 2013, **7**, 10190-10196.

39. Y. Wang, W. Ding, S. Chen, Y. Nie, K. Xiong and Z. Wei, *Chem. Commun.*, 2014, **50**, 15529-15532.

40. M. Yang, X. Hu, Z. Fang, L. Sun, Z. Yuan, S. Wang, W. Hong, X. Chen and D. Yu, *Adv. Funct. Mater.*, 2017, **27**, 1701971.

41. C. Tang, B. Wang, H.-F. Wang and Q. Zhang, *Adv. Mater.*, 2017, **29**, 1703185.

42. J. Zhang, Z. Zhao, Z. Xia and L. Dai, *Nat Nano*, 2015, **10**, 444-452.

43. J. Yang, H. Sun, H. Liang, H. Ji, L. Song, C. Gao and H. Xu, *Adv. Mater.*, 2016, **28**, 4606-4613.

44. Q. Liu, Y. Wang, L. Dai and J. Yao, *Adv. Mater.*, 2016, **28**, 3000–3006.

45. Q. Liu, Y. Wang, L. Dai and J. Yao, *Adv. Mater.*, 2016, **28**, 3000-3006.

46. M. Prabu, K. Ketpang and S. Shanmugam, *Nanoscale*, 2014, **6**, 3173-3181.

47. X. Liu, M. Park, M. G. Kim, S. Gupta, X. Wang, G. Wu and J. Cho, *Nano Energy*, 2016, **20**, 315-325.

48. Y. Jin and F. Chen, *Electrochim. Acta*, 2015, **158**, 437-445.

49. Y. Li, M. Gong, Y. Liang, J. Feng, J.-E. Kim, H. Wang, G. Hong, B. Zhang and H. Dai, Nat. Commun., 2013, **4**, 1805.

50. G. Fu, Z. Cui, Y. Chen, Y. Li, Y. Tang and J. B. Goodenough, *Adv. Energy Mater.*, 2017, **7**, 1601172.